

# STEREOSCOPIC 3D-IMAGE SEQUENCE ANALYSIS OF SEA SURFACES

F. Santel, W. Linder, C. Heipke

Institute of Photogrammetry and GeoInformation, University of Hannover,  
Nienburger Straße 1, 30167 Hannover, Germany  
(santel, linder, heipke)@ipi.uni-hannover.de

## Inter-Commission V/III

**KEY WORDS:** Matching, Sequences, Sea, Surface, Reconstruction, Video, Stereoscopic, Three-dimensional

### ABSTRACT:

Numerical modelling of highly complex processes in the surf and swash zone is an important task in coastal zone management. As input and reference data for these numerical models three-dimensional information about the water surface is required. In this paper a method for reconstructing a dynamic digital surface model of a surf zone based on stereoscopic image sequences is presented. The surface model is obtained by digital image matching using a variation of the vertical line locus method. The processing principles for stereoscopic image sequence analysis and the results are described. The image matching is checked by manual stereo analysis and gauge data. The research area is a groyne field on a North Sea island in Germany.

## 1. INTRODUCTION

In coastal zone management the optimisation of constructions like dykes or groynes is of high interest. The design of their shape and surface properties requires detailed information about the waves attacking them. In this context monitoring and prediction of the sea state in the surf zone is very important. The processes in the surf zone, like wave breaking, wave runup and wave overtopping can be described by numerical modelling (e.g. Strybny, Zielke, 2000). The geometric shape of the water surface is an important element for the numerical models. However, currently only point-wise gauge and buoy measurements are available to control such models.

In principle the water surface model can be provided with the required temporal and spatial resolution for the calibration and validation of the numerical model using digital photogrammetry (Strybny et al., 2001). Digital image matching was already employed successfully for the determination of wave parameters from stereo images in the past (e.g. Redweik, 1993). Further examples for the determination of sea surfaces using stereo images are given in Holland et al. (1997), Taguchi, Tsuru (1998) and Yamazaki et al. (1998).

The goal of our work is the three-dimensional and quasi-continuous determination of the water surface in the surf zone using an automatic photogrammetric approach. The approach processes stereoscopic video image sequences by image matching.

The analysis of image sequences is a challenging problem and has been an important research topic in the areas of photogrammetry and computer vision for some time. Horn (1986) for example used optical flow to determine the motion of a camera from an image sequence. An algorithm obtaining a three-dimensional model from image sequences is presented by Pollefeys et al. (2000). The system is able to extract automatically a textured three-dimensional surface from an image sequence without prior knowledge about the scene or the camera. In our case image sequence analysis is used for the

surface determination of a dynamic process, i.e. the tracking of a moving surface with static cameras.

## 2. IMAGE MATCHING

The computation of a digital surface model from images requires the interior and the exterior orientation of the images as well as homologous points. Assuming the orientation to be given, the identification and the image coordinate measurement of homologous points in two or more overlapping images via image matching over time remains the major task to be solved.

### 2.1 Point-wise Correlation

The three-dimensional determination of the water surface is accomplished by digital image matching using stereoscopic images as implemented in the software package LISA (Linder, 2003). By successive point-wise matching based on cross correlation over the model area through a sophisticated region growing algorithm starting from given seed points, a three-dimensional point cloud is generated, subsequently a digital surface model (DSM) is obtained by interpolation.

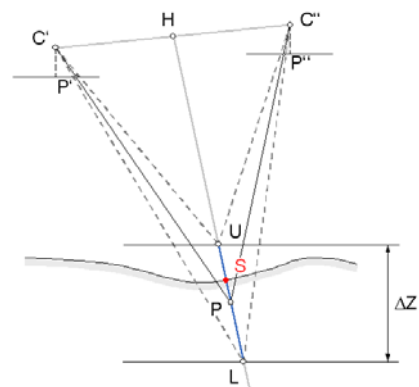


Figure 1. Point-wise matching algorithm

The point-wise matching algorithm runs as follows: Approximate three-dimensional coordinates for the seed point P, the maximum height variation  $\Delta Z$  in object space and orientations of the images are needed as input data. A straight line is then defined through the centre H of the camera base C'C'' and the seed point P (see Figure 1). Also the uppermost point U, which lies  $\Delta Z/2$  above P, and the lowermost point L, which lies  $\Delta Z/2$  below P, lie on this line. Between U and L several points are defined in a way that their distance in image space amounts to approximately one pixel.

Using the collinearity equations all these points are then projected into image space yielding several point pairs (P', P''). Square windows of a predefined size are set up around each position in the left image. The window in the right image is defined by projecting the four corners of the window in the left image into object space and then into the right image, in both cases using the central perspective transformation. For each pair of windows the cross correlation coefficient  $\rho$  is computed. The window pair with the maximum coefficient  $\rho_{max}$  is considered to be the pair of conjugate points corresponding to the point S in object space (see again Figure 1), provided that  $\rho_{max}$  lies above a pre-specified threshold value. Otherwise the point is rejected.

In order to exclude incorrect correlations, due to small contrast for example,  $\rho_{max}$  is also checked for uniqueness: From the neighbouring five correlation coefficients on either side, the minimum value  $\rho_{min}$  is selected. If the difference between  $\rho_{max}$  and  $\rho_{min}$  is smaller than a value of 0.5, the object point is rejected.

The described principle of point-wise correlation can be considered as a variety of the method of vertical line locus (Bethel, 1986). The difference is that points are selected on the line HP rather than a vertical line through P.

## 2.2 Region Growing

A three-dimensional point cloud is generated continuing the point-wise correlation over the entire model area by region growing. Region growing is divided into two parts.

First, the original images are down-sampled. Then, rays in the XY-plane are defined starting from each seed point into the eight main directions. Using a constant step size in X and Y direction, points on these rays are selected. The step size is taken to be equivalent to the grid size of the DSM to be eventually generated. Starting from the results of the seed points, point-wise correlation on the reduced image resolution is carried out for each new point on the rays, always using the Z value of the previous point as initial height value. Region growing in each direction and for each seed point continues until the correlation fails.

In the next step a regular DSM is interpolated from the resulting three-dimensional points, and point-wise correlation is repeated for each grid node using the original images. Finally, the results are low-pass filtered to eliminate gross errors.

## 3. IMAGE SEQUENCE ANALYSIS

The basic idea of processing image sequences in our approach is that in the area of non-breaking waves the change in height of the DSM from one image to the next is very small. This value obviously depends on the recording frequency and must be chosen accordingly. It is then possible to start the process of image matching using only a few manually measured seed points (Santel et al., 2002). Our method is able to find the needed seed points of the following stereo pairs automatically.

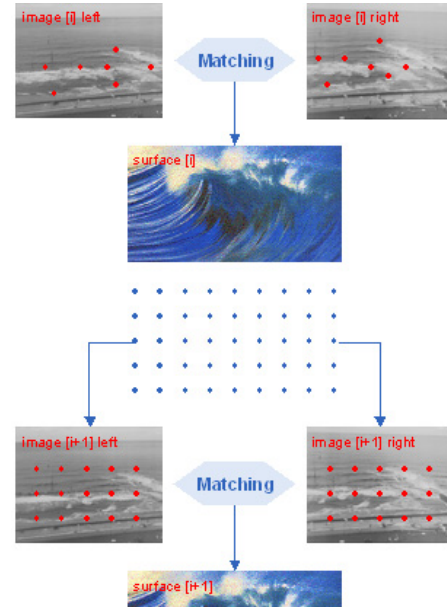


Figure 2. Determination of wave surfaces from image Sequences

In the following the analysis of image sequences is described in more detail (see Figure 2). The matching procedure is executed for the first stereo pair at time step [i]. This leads to a large number of object points. Because of the small wave motion, the object points of the time step [i] can be utilized as seed points for the following time step [i+1]. In order to reduce the matching effort only a pre-specified amount of regularly spaced points generated at step [i] is used as seed points at [i+1]. Matching of the stereo images [i+1] is carried out. Then the results are used in the same way for the stereo images [i+2] and so on.

## 4. EXPERIMENTAL TEST

In order to test the described method for the envisaged applications we acquired four stereoscopic image sequences of the coast of Northern Germany using digital video cameras. The selected area is a groyne field seawards Norderney Island. The size is approximately 200 by 200 m<sup>2</sup>.

The background for the test, and indeed the project, is a cooperation with the Institute of Fluid Mechanics and Computer Applications in Civil Engineering, University of Hannover, with the aim to test the applicability of digital photogrammetry for the application at hand. The project is being carried out together with the local administration responsible for coastal management and protection.

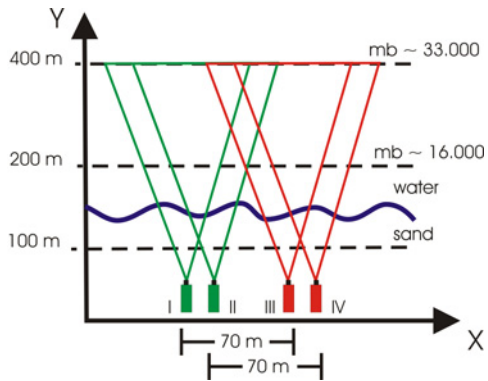


Figure 3. Camera constellation

The image acquisition was carried out from the top of two high buildings close to the groyne field. On each building two cameras were set up. Due to the altitude of the camera positions of about 40 m and a maximum distance of 400 m at the outer boundary of the area under investigation, the cameras point downwards with an angle of approximately 10 degrees. This camera constellation results in two overlapping stereo models I/II and III/IV (see Figure 3). The orientation of the images was established manually after image acquisition. The orientation parameters are assumed to be constant for the acquisition of an image sequence.

The centre of the area to be investigated has a distance from the cameras of approximately 200 m. At this distance the images have a scale of about 1 : 16 000. Assuming an accuracy of the image coordinates of 1 pixel (6.7  $\mu\text{m}$ ) in image space, a theoretical standard deviation of 10.7 cm in X and Z, and 142.9 cm in Y is obtained using standard error propagation formulae for the stereo pair I/II (see Figure 3). The poor accuracy in Y reflects the small stereo base. From the point of view of the application, however, the Z-accuracy is the most critical one.

## 5. RESULTS AND ACCURACY CHECKS

For the generation of the dynamic DSM approximately 100 well distributed seed points were measured manually in the first stereo pair of the image sequence I/II. Using these seed points approximately 20 000 conjugate object points were determined automatically by image matching. Subsequently, matching of a 5 min image sequence acquired with a frequency of 8 Hz was carried out as described in section 2 and 3. The sequence consists of 2 400 images.

In the following the image matching results are checked by manual analysis and gauge data. First the comparison with the manual measurement is carried out for one epoch and afterwards with the gauge data for multiple epochs.

### 5.1 One Epoch

Figure 4 shows the correlated points derived from the thirtieth stereo pair of the image sequence I/II and the associated orthophoto.

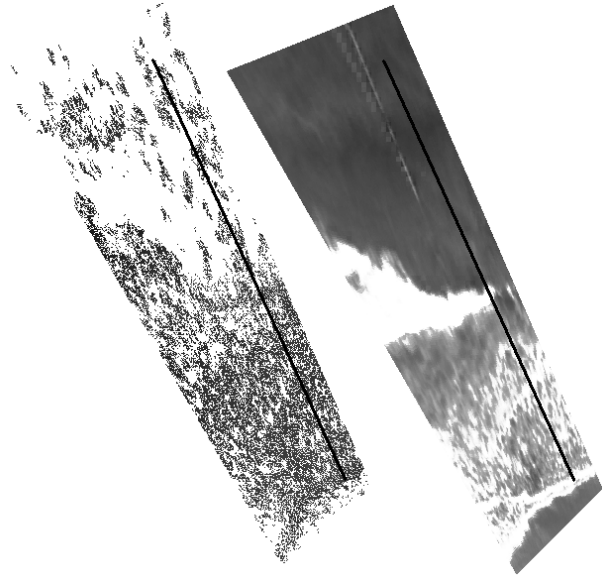


Figure 4. Correlated points and associated orthophoto

The image matching results were spot checked by manual stereo analysis. The manual stereo measurements have been carried out with the Image Station Z IV of Z/I Imaging. For some stereo pairs the DSM has been acquired twice. The standard deviation derived from double measurements amounts to approximately 10 cm in the surf zone, the results in the seawards area are slightly worse.

The manual measurement was undertaken for several stereo pairs of the image sequence. At each time a part of the entire matched area was analysed.

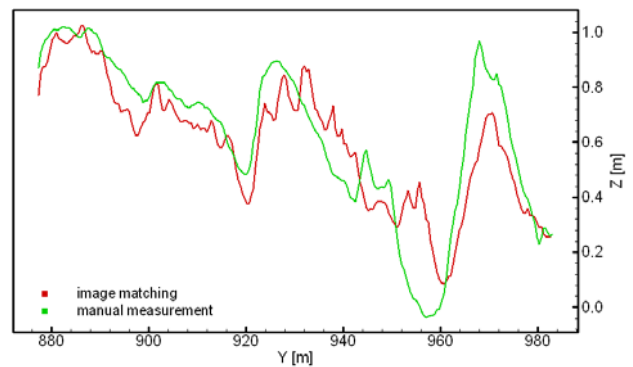


Figure 5. Comparison of image matching and manual measurement (Profile through the DSM)

Figure 5 shows a comparison of image matching and a manual measurement. The displayed data correspond to the profile highlighted in black in Figure 4. The profile represents a cross-section of the surf zone. Overall, the manual measurement is much smoother than the matching results. The beach is located at the left side of Figure 5. In the swash zone (Y = 892 m up to 913 m) slight differences between the manual measurement and the surface derived by image matching arise. The small wave in the surf zone (Y = 902 m) is well detected by image matching. Discrepancies occur at the breaking wave (Y = 927 m) due to the inexact determination at the sea spray. In the manual measurement clearly identifiable points on the sea surface or on the sea spray were captured. The matching algorithm, on the other hand, compares the grey values of the left matching

window and the grey values of the corresponding pixels of the right image resulting in somewhat different results. In addition, some errors appear in the seaward area because of the poor texture of the sea surface. The ripples ( $Y = 943$  m up to  $951$  m) as well as the trough of the sea ( $Y = 958$  m) are present in the matching result, however the wave at the outer seaward boundary ( $Y = 969$  m) can be distinguished, albeit with a wrong altitude.

The standard deviation between the two curves is  $9$  cm and thus in the same range as the analytically determined surface.

## 5.2 Multiple Epochs

Now we turn to the results of the image sequence analysis. Three derived water surfaces of the image sequence with a time difference of  $1$  s from epoch to epoch are illustrated in the left part of Figure 6. The positions of the wave peaks can be well identified and tracked in the surface models. Additionally produced orthophotos overlaid to the corresponding surfaces are shown in the right part of Figure 6. In both illustrations the wave positions coincide.

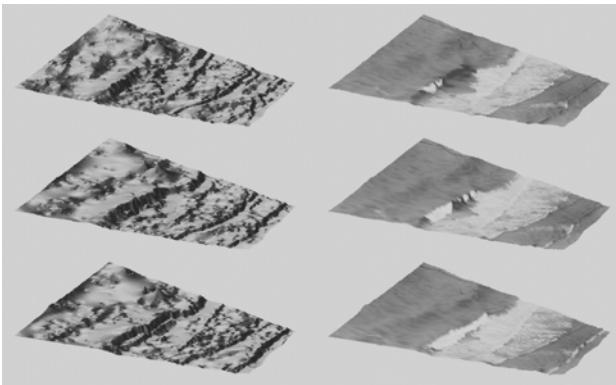


Figure 6. Sequence of water surfaces with  $\Delta t = 1$  s  
left: surface models; right: with overlaid orthophotos

During the measurement campaign at Norderney Island further measurements with conventional instruments, such as current meters, gauges and wave rider buoys have been carried out. From these point-wise measurements the altitude change of the sea surface can be derived. Using these data the developed procedure is also checked.

Figure 7 represents the image matching results at the position of one of the gauges and the gauge data over a period of  $56$  s. The  $56$  s are equal to a sequence of  $450$  images acquired with a frequency of  $8$  Hz. The horizontal axis of Figure 7 represents the time in MEZ. The vertical axis shows the height in metres. The analysed gauge is positioned at the centre of the area under investigation.

As can be seen, the height values determined by image matching corresponds to the gauge data in general. However, the image matching results show some high-frequency noise and problems arise in the areas of poor texture.

Also, some of the peak values of the two curves differ in the range of a few decimetres. It should be noted, that the standard deviation of the gauge data is not known in detail and is estimated to be in the decimetre range.

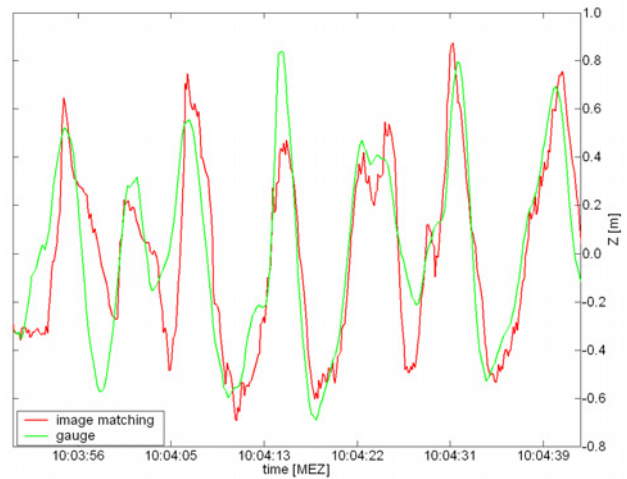


Figure 7. Comparison of image matching results and gauge data

In order to further analyse the differences between the matching results and the gauge measurements two time steps are compared exemplarily. These are time  $10:03:58$  and time  $10:04:21$ .

At time  $10:03:58$  the gauge is located in a trough of the sea. Here a difference of approximately  $35$  cm between the image matching result and the gauge data occur. This difference corresponds to  $3.3$  pixel in image space. When further investigating this results, we found that the grey value average of the matching window amounts  $74.1$  with a standard deviation of  $4.8$ . The mismatch thus occurred due to the poor texture of the sea surface. The limits of the algorithm are reached.

At time  $10:04:21$  matching is carried out in the swash zone of the following breaking wave. The difference between the image matching and the gauge data is less than  $5$  cm. In this case the corresponding matching window has a grey value average of  $186.6$  with a standard deviation of  $15.0$ . The image matching succeeds.

## 6. CONCLUSIONS

The determination of the water surface was carried out by digital image matching in object space. An algorithm for image sequence analysis was presented.

Experiments of the developed procedure demonstrate the successful derivation of area-wide and dynamic surface models of sea surfaces. The analysis of individual stereo models as well as of image sequences is feasible. The image matching results were spot-checked by manual stereo analysis and by the comparison with gauge data and were found to be accurate within the expectations.

Further adjustments of the matching algorithm to the specific problems of water surface modelling and the optimisation of the parameter choice will be tackled as one of the next steps, including tests for reducing the high-frequency noise still contained in the matching results. Finally the analysis of the entire groyne field will be achieved by combining the two overlapping stereo models.

The final DSM will then be used by the fluid mechanics group of our university as input and reference data for the numerical models. The results of this step will finally show whether our approach of combining digital photogrammetry and fluid dynamics for surf zone modelling is useful for practical applications.

## 7. REFERENCES

Bethel, J., 1986. The DSR11 Image Correlator. *American Congress on Surveying and Mapping, American Society of Photogrammetry and Remote Sensing*. Annual Convention, Vol. IV, pp. 44-49.

Holland, T., Holman, R. A., Lippmann, T. C., Stanley, J., 1997. Practical Use of Video Imagery in Nearshore Oceanographic Field Studies. *IEEE Journal of Oceanic Engineering*, 22(1), pp. 81-92.

Horn, B., 1986. *Robot Vision*. The MIT Press, Cambridge, Massachusetts.

Linder, W., 2003. *Digital Photogrammetry – Theory and Applications*. Springer-Verlag Berlin Heidelberg New York.

Pollefeys, M., Koch, R., Vergauwen, M., Van Gool, L., 2000. Automated reconstruction of 3D scenes from sequences of images. *ISPRS Journal of Photogrammetry & Remote Sensing*, (55)4, pp. 251-267.

Redweik, G., 1993. Untersuchungen zur Eignung der digitalen Bildzuordnung für die Ableitung von Seegangparametern. *Wissenschaftliche Arbeiten der Fachrichtung Vermessungswesen der Universität Hannover*, Nr. 194.

Santel, F., Heipke, C., Könnecke, S., Wegmann, H., 2002. Image Sequence Matching for the Determination of three-dimensional Wave Surfaces. *International Archives of Photogrammetry, Remote Sensing and Spatial Information Sciences*, Vol. XXXIV, Part 5, pp. 596-600.

Strybny, J., Wegmann, H., Santel, F., 2001. Combining Phase-Resolving Wave Models with Photogrammetric Measurement Techniques. In: *Ocean Wave Measurement and Analysis, American Society of Civil Engineering*, Vol. I, pp. 191-200.

Strybny, J., Zielke, W., 2000. Extended Eddy Viscosity Concept for Wave Breaking in Boussinesq Type Models, *Proceedings of the 27<sup>th</sup> International Conference on Coastal Engineering (ICCE)*. *American Society of Civil Engineers*, Vol. 2, pp 1307-1320.

Taguchi, T., Tsuru, K., 1998. Analysis of Flood by Stereomatching Method. *International Archives of Photogrammetry and Remote Sensing*, Vol. XXXII, Part 5, pp. 810-813.

Yamazaki, F., Hatamoto, M., Kondo, M., 1998. Utilization of Synchronous Shutter Apparatus in the Photographic Measurement Method of Flood Flow Surfaces. *International Archives of Photogrammetry and Remote Sensing*, Vol. XXXII, Part 5, pp. 848-855.

## 8. ACKNOWLEDGEMENTS

The presented work is part of the project WaveScan. WaveScan is a collaboration between the Institute of Photogrammetry and GeoInformation (IPI) and the Institute of Fluid Mechanics and Computer Applications in Civil Engineering (ISEB), both University of Hannover. The authors are grateful to the Federal Ministry of Education and Research (BMBF) and the German Coastal Engineering Research Council (KFKI) for funding under the project contract no. 03KIS026, and also for the advice and support received from the Lower Saxony Water Management and Coastal Defence Agency (NLWK) Norden and from the Coastal Research Center (FSK) Norderney of the Lower Saxony State Office for Ecology (NLÖ).